The Relative Humidity in an Isentropic Advection–Condensation Model: Limited Poleward Influence and Properties of Subtropical Minima

PAUL A. O'GORMAN

Massachusetts Institute of Technology, Cambridge, Massachusetts

NICOLAS LAMQUIN* AND TAPIO SCHNEIDER

California Institute of Technology, Pasadena, California

MARTIN S. SINGH

Massachusetts Institute of Technology, Cambridge, Massachusetts

ABSTRACT

An idealized model of advection and condensation of water vapor is considered as a representation of processes influencing the humidity distribution along isentropic surfaces in the free troposphere. Results are presented for how the mean relative humidity distribution varies in response to changes in the distribution of saturation specific humidity and in the amplitude of a tropical moisture source. Changes in the tropical moisture source are found to have little effect on the relative humidity poleward of the subtropical minima, suggesting a lack of poleward influence despite much greater water vapor concentrations at lower latitudes. The subtropical minima in relative humidity are found to be located just equatorward of the inflection points of the saturation specific humidity profile along the isentropic surface. The degree of mean subsaturation is found to vary with the magnitude of the meridional gradient of saturation specific humidity when other parameters are held fixed.

The atmospheric relevance of these results is investigated by comparison with the positions of the relative humidity minima in reanalysis data and by examining poleward influence of relative humidity in simulations with an idealized general circulation model. It is suggested that the limited poleward influence of relative humidity may constrain the propagation of errors in simulated humidity fields.

1. Introduction

The humidity distribution of the free troposphere plays an important role in the climate system for a number of reasons. Much attention has focused on the effect of upper-tropospheric water vapor on radiative transfer (Pierrehumbert 1995; Held and Soden 2000). But the humidity distribution of the free troposphere also plays an important role in determining the distributions of clouds (e.g., Mitchell and Ingram 1992) and precipitation

(e.g., Derbyshire et al. 2004). Although there has been much progress in our understanding of how the distribution of relative humidity arises (Sherwood et al. 2010b), this is still not well understood because of the complicated effects of condensation and moist convection. Here we further develop our basic understanding of the relative humidity distribution. In the limited context of a model of advection and condensation on isentropic surfaces, we ask: How do relative humidity minima in the subtropics arise? What determines the positions and magnitudes of the subtropical relative humidity minima? To what extent does the relative humidity in one region (e.g., the deep tropics) affect the relative humidity in other regions (e.g., in the subtropics or higher latitudes)? Answers to these questions can be expected to be helpful for the climate change problem and for understanding the extent to which model errors in one region can affect the relative humidity in other regions. A broader understanding of

---

* Current affiliation: ACRI-ST, Sophia-Antipolis CEDEX, France.

Corresponding author address: Paul A. O'Gorman, Massachusetts Institute of Technology, 77 Massachusetts Avenue, Cambridge, MA 02139.
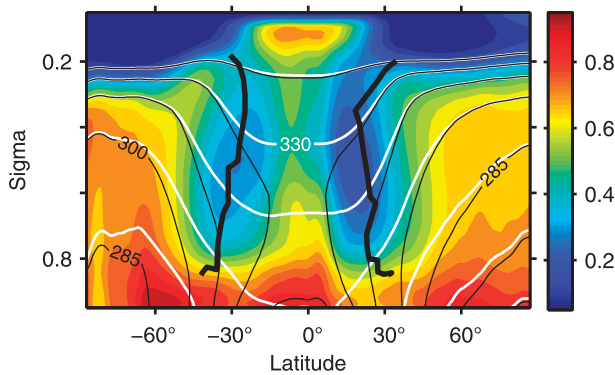E-mail: pog@mit.edu

FIG. 1. Zonal- and temporal-mean relative humidity (RH; color shading), dry potential temperature (white contours with interval = 15 K), and equivalent potential temperature (black contours with interval = 15 K) for DJF in the ERA-40 1980–2001. Potential temperature contours above 345 K are not shown. Equivalent potential temperature is evaluated using the approximate formula of Bolton (1980). Thick black lines show the locations of the inflection points of mean saturation specific humidity on dry isentropic surfaces, calculated using an isentropic vertical coordinate and then interpolated to a σ vertical coordinate. The inflection points shown correspond to the maximum rate of poleward decrease in mean saturation specific humidity on a given isentrope in each hemisphere. They are not shown above the tropopause or below $\sigma = 0.85$.

controls on the relative humidity distribution is expected to be helpful, for example, for understanding the humidity distribution of possible exoplanets with a hydrological cycle.

Factors that control the positions and values of the subtropical relative humidity minima will be a focus of our study. The minima occur in the zonal- and temporal-mean relative humidity of each hemisphere, as shown in Fig. 1, which is based on the 40-yr European Centre for Medium-Range Weather Forecasts (ECMWF) Re-Analysis (ERA-40; Uppala et al. 2005). The importance of these relatively dry regions has been emphasized for the maintenance of the climate state and for how it might respond to climate change (Pierrehumbert 1995; Held and Soden 2000). One approach to understanding what controls the subtropical humidity is to analyze the water vapor budget of the region in dry isentropic coordinates. Although there is a strong isentropic flux through the positions of the relative humidity minima, it is almost nondivergent in the zonal and temporal mean, leaving a balance between drying owing to cross-isentropic mean subsidence and moistening owing to convection (Schneider et al. 2006; Couhert et al. 2010). A different perspective on humidity maintenance comes from the method of "tracers of last saturation" (Galewsky et al. 2005; Wright et al. 2010; Hurley and Galewsky 2010a,b). This is a variant of the advection–condensation modeling approach in which air parcels are advected by the large-scale wind and conserve their

specific humidity except when a grid-scale saturation limit is exceeded (Sherwood 1996; Salathé and Hartmann 1997; Pierrehumbert and Roca 1998; Dessler and Sherwood 2000). The results suggest that more than half of the air at the subtropical relative humidity minima was last saturated poleward of the minima on the mean dry isentropic surface intersecting the minima, consistent with dehydration by eddy motions of air parcels that are nearly isentropic (Yang and Pierrehumbert 1994; Galewsky et al. 2005). However, the frequency distribution of last saturation location must be weighted by the saturation specific humidity distribution to determine the contribution to mean specific humidity. Moist air coming from the lower troposphere with a high saturation specific humidity also contributes to the subtropical specific humidity near the relative humidity minima (Galewsky et al. 2005; Schneider et al. 2006) and is a primary contributor to the increased specific humidity there seen in global warming simulations (Hurley and Galewsky 2010b). Simulated changes in relative humidity in response to global warming are found to be smaller than the fractional changes in specific humidity, but they nonetheless have a consistent pattern in different climate models (Mitchell and Ingram 1992; Sherwood et al. 2010a) and have been related to shifts in the circulation and changes in the frequency distribution of last saturation locations (Wright et al. 2010).

The maintenance and changes of the humidity field, then, involve a number of interacting physical processes. To gain insights into how the relative humidity is maintained in a more idealized setting, Pierrehumbert et al. (2007) introduced a version of advection–condensation modeling in which the advecting winds are taken to be stochastic processes. O'Gorman and Schneider (2006) extended the approach to more general stochastic wind processes and linked the stochastic model to simulations with turbulent velocity fields. They considered a prototype setting with a monotonic saturation specific humidity profile and without spatially inhomogeneous moisture sources. They also derived differential equations governing the mean relative humidity distribution and found that the nonlocality introduced by condensation was manifested in a dependence on the meridional "distance to saturation" of air parcels.

In this paper, we follow the idealized approach of Pierrehumbert et al. (2007) and O'Gorman and Schneider (2006). Extending the earlier studies, we focus on a statistically steady state with an isentropic saturation humidity profile representative of the zonal-mean state of the atmosphere and with a spatially inhomogeneous moisture source that is largest in the region with highest water vapor concentrations (representative of the tropics).

The advection–condensation models we use are described in section 2. Simulations with default parameters

are described in section 3, followed by descriptions of three sets of sensitivity experiments. We investigate the extent to which nonlocal influences affect the relative humidity field by varying the magnitude of the tropical evaporation source in section 4. We investigate what controls the positions of the relative humidity minima by varying the shape of the saturation specific humidity profile in section 5. And we investigate what controls the relative humidity at the minima by varying the pole-to-equator difference in saturation specific humidity in section 6. Our results regarding the poleward influence of relative humidity are evaluated using simulations with an idealized general circulation model (GCM) in section 7, and our results are summarized and further discussed in section 8.

2. Methods

a. Model setup

As in O'Gorman and Schneider (2006), we consider a two-dimensional advection–condensation system as an idealized representation of eddy moisture transport along an isentropic surface in the free troposphere. We consider two types of advecting velocities: advection by simulated homogeneous and isotropic turbulent velocity fields and advection by velocity fields represented as stochastic processes. The stochastic velocity fields are more easily amenable to analysis, but it is important that similar results are obtained with the more realistic turbulent velocity fields. The present work extends that of O'Gorman and Schneider (2006) by considering moisture fields in statistical equilibrium with spatially inhomogeneous evaporation and saturation profiles. The moisture tracer is taken to be passive and does not affect the advecting flow through latent heat release or radiative effects. Condensation instantaneously prevents supersaturation with respect to a saturation distribution that is zonally symmetric and constant in time. Statistical equilibrium is reached by applying an evaporation source that is also zonally symmetric and constant in time.

The domain extends from $-\pi$ to π in the meridional coordinate y. For convenience we will refer to the center of the domain ($y = 0$) as the equator and the edges of the domain as the poles. But it is important to bear in mind the idealized nature of the model. For example, the velocity statistics are homogeneous in space so that there are no localized storm tracks at midlatitudes.

The evaporation profile $e(y)$ is the sum of a background rate $e_b = 0.1$ and a Gaussian function centered at $y = 0$ with amplitude A, such that

$$e(y) = e_b + A \exp\left[-\left(\frac{y}{2\pi B}\right)^2\right], \qquad (1)$$

where $B = 0.1$ is held fixed. The default value of the amplitude of the tropical source is $A = 0.3$, but A is varied in one series of experiments to have the values 0.01, 0.1, 0.3, and 0.7 (Fig. 3a).

The saturation specific humidity profile $q_s(y)$ is given by

$$q_s(y) = \alpha + \beta \tanh\left(\frac{y_0 - |y|}{\gamma\pi}\right), \qquad (2)$$

with

$$\alpha = q_s^e - \beta \tanh\left(\frac{y_0}{\gamma\pi}\right), \qquad (3)$$

$$\beta = \frac{q_s^e - q_s^p}{\tanh(y_0/\gamma\pi) - \tanh[(y_0 - \pi)/\gamma\pi]}, \qquad (4)$$

where $\gamma = 0.15$ is held fixed. The saturation specific humidity has a maximum value of $q_s^e = 0.8$ at the center of the domain (representative of the equator or where the isentropic surface reaches the surface). It monotonically decreases to a value of q_s^p at the boundaries of the domain (representative of higher latitudes where the isentropic surface reaches the tropopause or polar regions). The parameter y_0 controls the positions of the inflection points ($\pm y_0$) and is varied to have the values $\pi/2$, $2\pi/5$, $\pi/3$, and $\pi/4$ in one series of experiments (Fig. 6a); its default value is otherwise $y_0 = \pi/2$. The polar specific humidity q_s^p is varied to have the values 0.01, 0.1, 0.3, 0.5, and 0.7 in another series of experiments (Fig. 8a); its default value is otherwise $q_s^p = 0.01$. The saturation specific humidity profile is chosen to qualitatively resemble the sharp decrease in saturation specific humidity going from the warm tropics poleward along a mean dry isentropic surface, toward higher altitudes and latitudes (cf. the 330-K dry isentrope in Fig. 1). However, it may be argued that moist isentropic surfaces are the relevant isentropic surfaces in an atmosphere with latent heating, and so our model may also be considered to represent advection and condensation along surfaces of constant equivalent potential temperature (cf. the 330-K surface of equivalent potential temperature in Fig. 1).

b. Turbulent advection

In the version of the model in which the advecting velocity is a simulated two-dimensional turbulent flow, the evolution equation for the specific humidity $q(\mathbf{x}, t)$ is given by

$$\frac{\partial q}{\partial t} + \mathbf{u} \cdot \nabla q = e - c + \mathcal{F}, \qquad (5)$$

where $\mathbf{x} = (x, y)$ is the position, with zonal coordinate x and meridional coordinate y, $\mathbf{u} = (u, v)$ is the two-dimensional

advecting velocity, and $\mathcal{F}$ is a filter that damps only at small scales. The condensation term $c(\mathbf{x}, t)$ acts at each time step to prevent supersaturation where it would otherwise occur. The domain is a doubly periodic square of length 2π. The periodic boundary condition in the y direction is slightly inconsistent with the saturation specific humidity profile $q_s(y)$, but the discontinuity in the first derivative is relatively small (Fig. 6a) and does not cause substantial numerical problems in the simulations presented here.

The turbulent velocity field is incompressible, forced by a random Markov process, and damped by Rayleigh drag and a smoothing filter. The governing equations of the velocity field are the same as in O'Gorman and Schneider (2006), but we use a different set of forcing and damping parameters to obtain a velocity field with smaller eddies relative to the size of the domain. We use forcing localized at wavenumbers $6 \leq k \leq 7$ (rather than $2 \leq k \leq 4$), where k is the magnitude of the two-dimensional wavenumber vector. We also use double the spatial resolution (256^2) and twice the Rayleigh drag coefficient [0.6 in units of inverse model time; the eddy time scale based on enstrophy defined as in O'Gorman and Schneider (2006) is 0.78]. The smoothing filter $\mathcal{F}$ is applied to both the vorticity and the moisture fields and is only active at $k \geq 50$ (Smith et al. 2002; O'Gorman and Schneider 2006). The kinetic energy spectrum peaks at the forcing wavenumbers and displays a power-law range at higher wavenumbers that is roughly consistent with the steepness of the spectrum found in observations of the troposphere at large scales (Boer and Shepherd 1983); however, the tropospheric spectrum results from a more complicated range of processes than just the nonlinear eddy–eddy interactions that are important in the turbulent flow considered here (Schneider and Walker 2006; O'Gorman and Schneider 2007).

c. Stochastic advection

In the version of the model in which the advecting velocity is a stochastic process, the advection–condensation system is reduced to one spatial dimension y and written in Lagrangian form as

$$\frac{dq(Y, t)}{dt} = e(Y) - c(Y, t), \qquad (6)$$

where the Lagrangian position $Y(t)$ of an air parcel evolves according to

$$\frac{dY(t)}{dt} = V(t). \qquad (7)$$

The Lagrangian velocities $V(t)$ of air parcels are taken to be independent, identically distributed Ornstein–Uhlenbeck

processes with stationary statistics and zero mean. Similar stochastic models have been used extensively to study dispersion of passive scalars in a turbulent flow (e.g., Thomson 1987). The two-time autocorrelation of each velocity is given by

$$\overline{V(t)V(t')} = \overline{v^2} \exp(-|t - t'|/\tau), \qquad (8)$$

where τ is the Lagrangian velocity correlation time and $\overline{(\cdot)}$ denotes an ensemble or time average. The velocity variance and Lagrangian velocity correlation time are chosen to match the statistics in the two-dimensional turbulence velocity field, with $\overline{v^2} = 0.83$ and $\tau = 0.29$. The domain is again periodic in y and of length 2π. In O'Gorman and Schneider (2006), it was found to be necessary to take into account the effect of small-scale dissipation of moisture variance in order to obtain good agreement with the moisture statistics obtained from the two-dimensional turbulence model with a smoothing filter. But the saturation humidity profiles used here are a stronger constraint on the moisture variance than were the periodic linear profiles used in O'Gorman and Schneider (2006), and we find that we can neglect small-scale dissipation of moisture variance in the stochastic version of the model here.

d. Averages

The mean used is a temporal and zonal mean for the turbulence simulations and a temporal and particle mean for the stochastic simulations. In the turbulence simulations, the velocity and moisture fields were run to statistical equilibrium, and statistics were then collected over a model time of 240 (greater than 300 eddy time scales). In the stochastic model, 2×10^5 particles were used and averages were taken over the particles and over a duration of 40 model time units after statistical equilibrium had been reached.

e. Theoretical guidance

Theoretical guidance in interpreting model results comes from analytical expressions derived by O'Gorman and Schneider (2006) for the mean moisture flux [(A1)] and mean condensation rate [(A2)]. The expressions are valid in the ballistic limit in which the Lagrangian velocity autocorrelation time is large compared with other relevant time scales (such as time scales associated with condensation). Similar expressions were also derived by O'Gorman and Schneider (2006) in the Brownian limit of small velocity autocorrelation times. The expressions for neither limit are directly applicable to the mean flux and mean condensation rate for the models we consider here, primarily because of the evaporation source and the finite correlation time of the advecting velocity, but
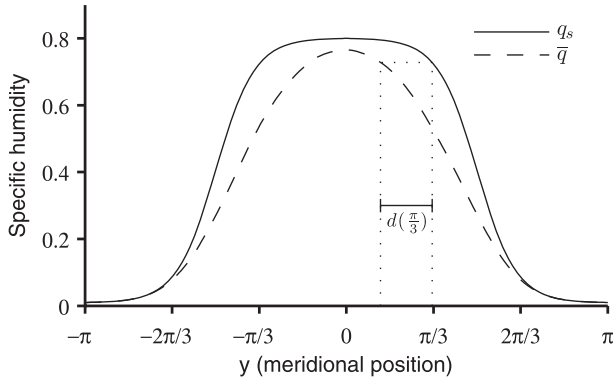
FIG. 2. Saturation specific humidity (solid line) and mean specific humidity (dashed line) in the turbulence model with default parameters ($A = 0.3$, $y_0 = \pi/2$, $q_s^p = 0.01$). Calculation of the distance to saturation $d(y)$ defined by (10) is illustrated for $y = \pi/3$ by the horizontal line segment that extends from $y' = \pi/3 - d(\pi/3)$ to $y = \pi/3$.

also because they require a monotonic specific humidity field in the meridional direction and were derived by assuming an initial condition for specific humidity rather than a statistical steady state. Nonetheless, the expressions do provide helpful qualitative guidance for the interpretation of results; for example, they show that the mean moisture flux is decreased by the presence of condensation, and that the mean condensation rate scales with the meridional gradient of saturation specific humidity.

The distance to saturation is an important variable that arises in the analytical expressions and in the model analysis. We define y' for a given meridional position y as the closest point at which the mean specific humidity at y' is equal to the saturation specific humidity at y:

$$\overline{q}(y') = q_s(y). \tag{9}$$

The distance to saturation is then defined as the distance between y and y':

$$d(y) = |y - y'|, \tag{10}$$

as illustrated in Fig. 2. It is independent of time because we consider steady-state solutions. The distance to saturation measures the distance an air parcel with the mean specific humidity must move poleward (in the absence of evaporation) to reach saturation at y. It may be viewed as a measure of subsaturation, with subsaturation increasing for greater distance to saturation. If there is no point y' within the domain with mean specific humidity equal to the saturation specific humidity at y, then we say that the distance to saturation is infinite at y.

We also make use of an exact solution of the advection–condensation problem for Brownian air parcels and a restoring humidity boundary condition at the

equator (Sukhatme and Young 2011) as described in appendix B.

3. Climatology with default parameters

Specific humidity and saturation specific humidity are shown for the default parameter settings ($A = 0.3$, $y_0 = \pi/2$, $q_s^p = 0.01$) in Fig. 2. Note that the model is statistically symmetric about the equator, and so any lack of such symmetry in the plots is indicative of sampling error. The relative humidity is defined here as the ratio of the specific humidity to the saturation specific humidity ($r \equiv q/q_s$). The mean relative humidity is close to one at the equator and at high latitudes (cf. Fig. 3b). The humidity must be close to saturation at high latitudes because there is no mechanism in the model to generate air that is subsaturated with respect to the minimum saturation specific humidity, which occurs at the poles. The default strength of the tropical evaporation source ($A = 0.3$) is sufficient to maintain a high relative humidity at the equator in the mean. Relative humidity minima are located near $|y| = \pi/2$. The value at the minima ($r \approx 0.66$) is not as low as the subtropical minima found in Earth's atmosphere in the zonal mean (Fig. 1). In Earth's atmosphere, other processes in addition to isentropic advection and condensation (e.g., subsidence of dry air from the upper troposphere) also influence the relative humidity in the subtropics.

The meridional moisture flux is poleward and reaches maximum magnitude just equatorward of $|y| = \pi/2$ (Fig. 3c). The closeness in position of the relative humidity minima and of the extrema in meridional moisture flux implies that the moisture flux divergence is relatively small near the relative humidity minima, as in Earth's atmosphere in the zonal mean (Schneider et al. 2006; Couhert et al. 2010). According to the expressions derived by O'Gorman and Schneider (2006), the moisture flux [(A1)] is proportional to the negative of the gradient in specific humidity if the distance to saturation [(10)] is large:

$$\overline{vq} \propto -\frac{\partial \overline{q}}{\partial y}. \tag{11}$$

Thus, if the distance to saturation is large and if fractional variations in relative humidity are smaller than fractional variations in saturation specific humidity, then the meridional moisture flux should have maximum magnitude near the inflection points of the saturation specific humidity profile (here at $|y| = y_0 = \pi/2$). The effect of condensation will be to decrease the moisture flux in regions of small distance to saturation, which will tend to push the moisture flux maxima equatorward of $\pm y_0$, since the distance to saturation decreases poleward (as shown in the next section). The shape of the relative humidity
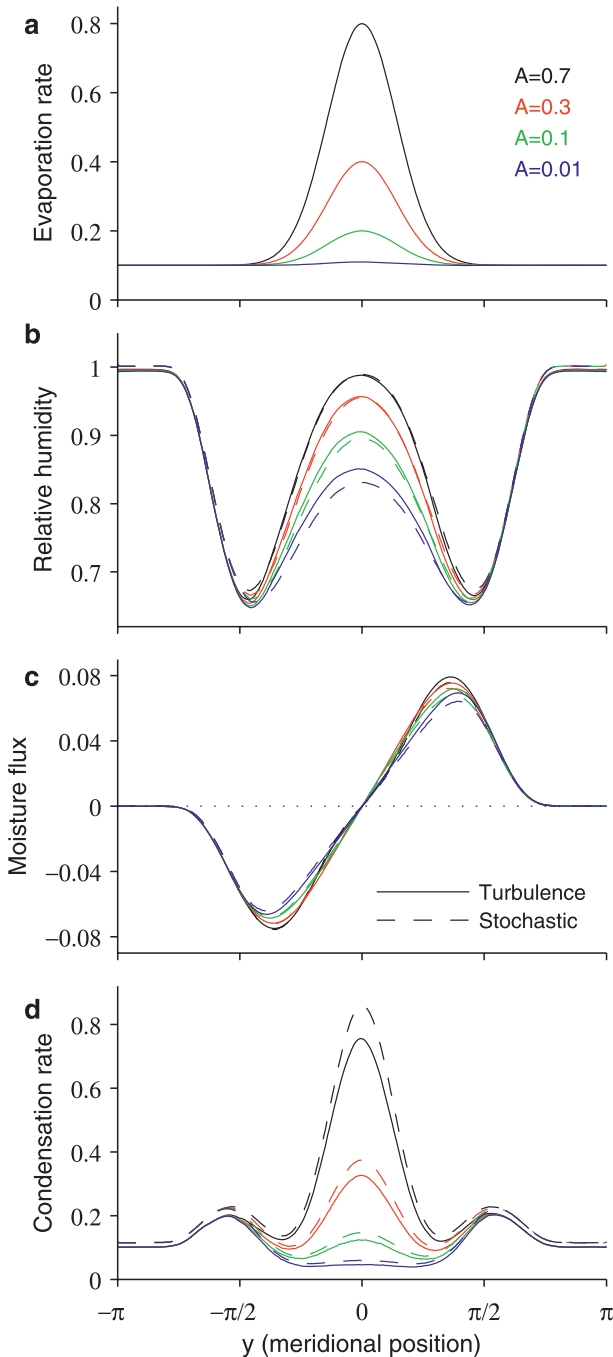
FIG. 3. (a) Variations in the strength of the tropical evaporation source (obtained by varying A), and the resulting mean fields in the turbulence model (solid lines) and stochastic model (dashed lines): (b) RH, (c) meridional specific humidity flux, and (d) condensation rate.

profile must also be taken into account (since fractional variations in relative humidity are only negligible sufficiently far poleward), and this also helps explain why the moisture flux maxima are equatorward of $\pm y_0$.

Local maxima in the condensation rate occur at the equator (related to the maximum in evaporation rate there) and just poleward of the relative humidity minima (Fig. 3d). According to the expression for the mean condensation rate [(A2)], the condensation rate (in the absence of evaporation) should be proportional to the gradient in saturation specific humidity dq_s/dy and should be monotonically increasing with decreasing distance to saturation. The dependence on dq_s/dy alone would imply midlatitude maxima in condensation rate at the inflection points of the saturation specific humidity profile at $y_0 = \pm\pi/2$. The dependence on distance to saturation pushes the maxima poleward of $\pm y_0$.

There is good agreement between the turbulence and stochastic versions of the model in all fields considered. The largest discrepancy occurs in the condensation rate, with a somewhat larger condensation rate in the stochastic version of the model.

We next consider three series of experiments in which the evaporation source strength and parameters controlling the shape of the saturation specific humidity profile are independently varied.

4. Limited poleward influence of relative humidity

The question of the extent to which the relative humidity in the tropics affects the relative humidity at higher latitudes is addressed by analyzing simulations in which the strength A of the evaporation source in the tropics is varied (Fig. 3a). We are concerned here only with influence through moisture transports, and not indirect effects through radiation or latent heat release (which would affect the saturation specific humidity).

As A is varied from 0.01 to 0.7, the relative humidity at the equator monotonically increases in value from $r \simeq 0.85$ to 1.0 (Fig. 3b). But the influence of these changes on the relative humidity at higher latitudes is slight. In fact, there are almost no changes in relative humidity poleward of $|y| = \pi/2$, as shown in close-up in Fig. 4, which includes only results from the turbulence model for clarity. A similarly sharp convergence of the relative humidity profiles occurs in the stochastic model. The relative humidity minima occur at latitudes at which there is a detectable response to the variations in the tropical evaporation source amplitude, but the changes in the minimum relative humidity values are only of order 0.01 over the entire range of simulations. Consistent with the invariance of the relative humidity poleward of $|y| = \pi/2$, the moisture flux and condensation rate poleward of $|y| = \pi/2$ are also largely unaffected by changes in the tropical evaporation source (Figs. 3c,d).

Why is there so little influence of low-latitude relative humidity on the high-latitude relative humidity? This
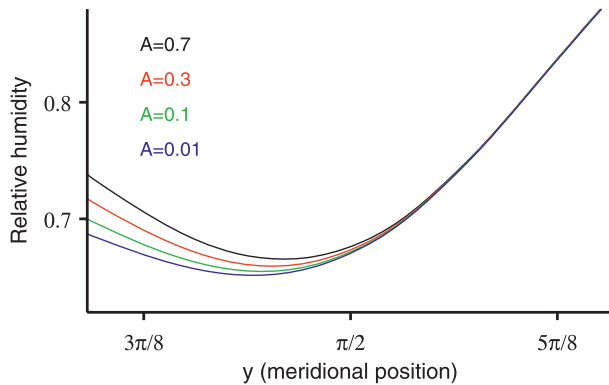
FIG. 4. Close-up of mean relative humidity near its minimum in the turbulence model for a range of values of the tropical evaporation source (cf. Fig. 3).

lack of influence would not occur in a simple diffusive system without condensation, especially given the much greater concentrations of water vapor at low latitudes. The inadequacy of diffusion to represent the kinematics of moisture transport and condensation has previously been pointed out in the closely related "cold trap" problem (Pierrehumbert et al. 2007). The effect of condensation is to cut off the influence of air parcels coming from lower latitudes, at least past a certain latitude.

To see why, first consider the limit in which the distance to saturation is small, as might occur if the meridional specific humidity gradient is large or the relative humidity is close to one. Air parcels moving poleward toward a point y (and upward along an isentropic surface) cool adiabatically, reach saturation, and begin to condense. By the time such air parcels reach y, they have the local saturation specific humidity at y and have lost the memory of their earlier specific humidity. (The model considered here is idealized in having a fixed dependence of saturation specific humidity on y, but similar considerations apply to the real atmosphere because there is a correlation between poleward motion and adiabatic cooling.) Air parcels moving equatorward toward a point y will not experience condensation and so retain information about specific humidities poleward of y. There is, therefore, an important asymmetry in information propagation between equatorward- and poleward-moving air parcels.

To examine this asymmetry more quantitatively, we neglect evaporation and consider the ballistic limit in which air parcels do not change their velocities on the time scale in question. If the specific humidity is given by $q_i(y)$ at time zero, the mean specific humidity $\overline{q}(y,t)$ at a point y and time t may be written in terms of the transition probability $p(y - y_i, t)$ of an air parcel having moved from y_i at time zero to y at time t:

$$\overline{q}(y,t) = \int dy_i \min[q_i(y_i), q_s(y)]p(y - y_i, t). \quad (12)$$

The minimum function takes account of condensation for air parcels that reach saturation prior to reaching y. The position y' at which $q_i(y') = q_s(y)$ is the dividing point between air parcels that retain their specific humidity on their way toward y and those that do not, and as such it demarcates the equatorward limit of the domain of dependence for the specific humidity at y (the region in which the specific humidity may affect the specific humidity at y). The distance to saturation $d(y) = |y' - y|$ controls the equatorward extent of the domain of dependence for the specific humidity at y. For sufficiently large distance to saturation (compared to the typical distance traveled by air parcels over the time scale in question), the system reverts to an advection or diffusion system without condensation and there will be an influence of moisture in both directions. For sufficiently small distance to saturation, there is no influence on the relative humidity from the relative humidity field farther equatorward.[1]

The distance to saturation (neglecting evaporation) is shown in Fig. 5 for the series of experiments in which the tropical evaporation source strength A is varied. In all cases, the distance to saturation is infinite in the tropical region and rapidly decreases near $|y| = \pi/2$, consistent with the lack of influence of the tropical evaporation source variations on relative humidities poleward of $|y| = \pi/2$ (Fig. 4).

In the simulations presented, the meridional position at which the influence of variations in A goes to zero is coincident with the position at which the variations in the evaporation source become small (Fig. 3). So it could be argued that it is the meridional extent of the variations in evaporation source that determines the meridional extent of variations in relative humidity. But we have also calculated the exact solution in the case of a restoring boundary condition for moisture at the equator and no evaporation source otherwise, using the integral solution derived by Sukhatme and Young (2011) for the Brownian limit (see appendix B). This exact solution shows that for a restoring boundary condition at the equator, the influence of the equatorial specific humidity extends only to the position at which the

---

[1] The distance to saturation also plays a key role in the expressions for the mean flux (A1) and condensation rate (A2). In the limit of small distance to saturation, these only depend on local derivatives of the humidity fields (rather than also directly depending on the specific humidity at lower latitudes), consistent with less poleward influence, although these expressions do not make clear that poleward influence is completely absent in the limit of vanishing distance to saturation.
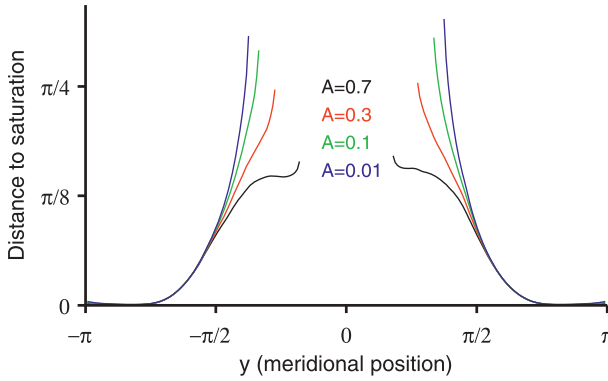
FIG. 5. Meridional distance to saturation for air parcels in the turbulence model over a range of values of the tropical evaporation source. The distance to saturation at y is defined by (10) in terms of the mean specific humidity and saturation specific humidity distributions (neglecting evaporation). The distance to saturation is not shown at locations at which it is infinite (i.e., locations with a higher saturation specific humidity than any mean specific humidity in the domain).

distance to saturation become infinite, consistent with condensation limiting the poleward influence of relative humidity. This exact solution also shows that limited poleward influence does not depend on the details of the saturation specific humidity profile, but it holds more generally.

5. Positions of the relative humidity minima

The question of what controls the meridional positions of the relative humidity minima is studied using a series of experiments in which the positions $\pm y_0$ of the inflection points of the saturation specific humidity profile are varied (Fig. 6a). As the inflection points move equatorward, the relative humidity minima also move equatorward at almost the same rate (Figs. 6b and 7). The midlatitude extrema of the meridional moisture flux and condensation rate similarly move equatorward (Figs. 6c,d). The minimum relative humidity value increases as it moves closer to the equator (Fig. 6b), possibly as a result of moving into the region of stronger evaporation.

As discussed earlier, it is unsurprising that the moisture flux should have maximum magnitude close to the inflection points $\pm y_0$ since this is where the saturation specific humidity gradient is largest in magnitude. But why do the relative humidity minima also occur close to $\pm y_0$? Consider first the case without evaporation and condensation in the region of the inflection points (although this is not a very good approximation for our simulations). At steady state and using the fact that the velocity statistics are spatially homogeneous in the model and that the moisture flux scales with the negative of the gradient of specific humidity in the absence of condensation [cf. (11)], we have
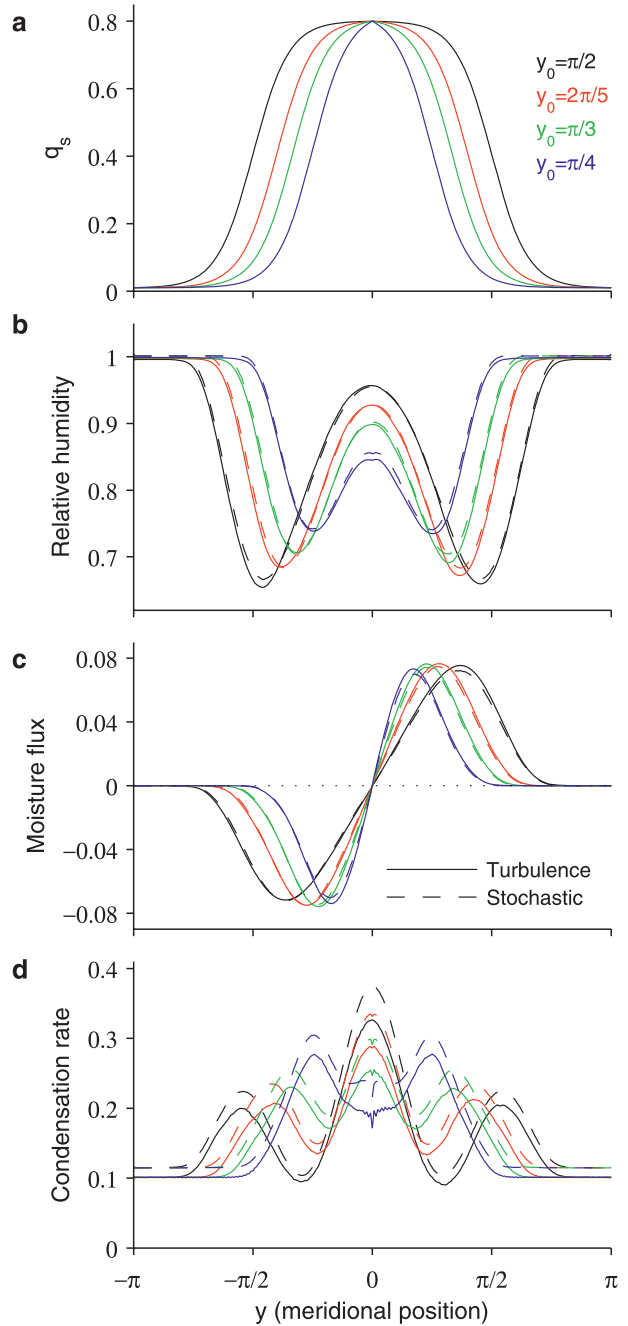

FIG. 6. (a) Variations in the positions $\pm y_0$ of the inflection points of saturation specific humidity, and the resulting mean fields in the turbulence model (solid lines) and stochastic model (dashed lines): (b) RH, (c) meridional specific humidity flux, and (d) condensation rate.

$$\frac{\partial^2 (\bar{r} q_s)}{\partial y^2} \approx 0, \qquad (13)$$

which may be rearranged to give an expression for the meridional gradient of relative humidity:
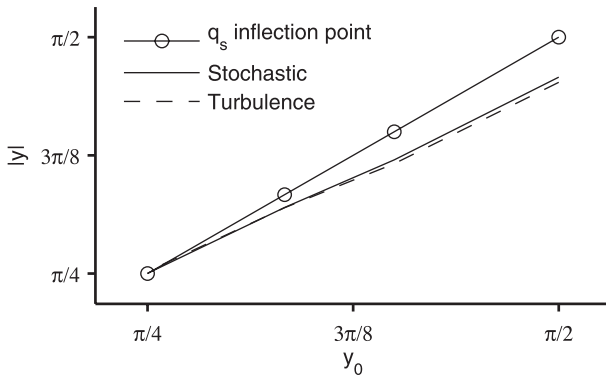
FIG. 7. Positions of the inflection points of saturation specific humidity (solid line and circles) and the RH minima in the stochastic model (solid line) and turbulence model (dashed line) for a range of positions $\pm y_0$ of the inflection points of saturation specific humidity.

$$\frac{\partial \overline{r}}{\partial y} \approx -\frac{\overline{q}}{2(dq_s/dy)}\left(\frac{1}{q_s}\frac{d^2 q_s}{dy^2} + \frac{1}{\overline{r}}\frac{\partial^2 \overline{r}}{\partial y^2}\right). \quad (14)$$

If the curvature of the relative humidity (the second term on the right-hand side) is negligible, the inflection points of saturation specific humidity are associated with extrema of relative humidity. The curvature of the relative humidity is positive at the relative humidity minima ($\partial^2 \overline{r}/\partial y^2 > 0$), so (14) actually implies that the relative humidity minima occur somewhat equatorward of the saturation specific humidity inflection point (in a region in which $d^2 q_s/dy^2 < 0$). The distance between the relative humidity minima and the q_s inflection points scales inversely with $d^3 q_s/dy^3$. It is small as long as fractional variations in q_s are large relative to fractional variations in relative humidity—which is the case in our simulations in the region of interest but is generally only a good approximation outside the tropics in Earth's atmosphere. This argument does not preclude there being a relative humidity minimum in the case that there are no inflection points of saturation specific humidity—for example, as found by Sukhatme and Young (2011) for an exponential saturation specific humidity profile.

In the more realistic case in which, for example, sources and sinks are nonnegligible and there are meridional variations in wind statistics and cross-isentropic vertical advection of air masses, it is no longer possible to reason about the positions of the minima using the simple arguments above. Nonetheless, we expect the positions of the minima to be strongly affected by the thermal structure of the atmosphere, since gradients of saturation specific humidity are key to the generation of subsaturated air by eddies. Figures 6b and 7 show that the relative humidity minima lie just equatorward of the inflection points in our

idealized model, with the distance between them decreasing as the inflection points move toward the equator. Similarly, Fig. 1 shows that the relative humidity minima lie close to (or just equatorward of) the inflection points of saturation specific humidity in the ERA-40 reanalysis in December–February (DJF) if the inflection points are calculated from the zonal- and temporal-mean saturation specific humidity in dry isentropic coordinates.[2] This is also the case in the idealized GCM simulations discussed in section 7.

On moist isentropic surfaces (surfaces of constant equivalent potential temperature) there is not necessarily an inflection point of saturation specific humidity in the middle troposphere, and the equivalent potential temperature tends to decrease with height in the lower troposphere (making it nonmonotonic and not suitable as a vertical coordinate). The applicability of the inflection point theory, therefore, depends on whether moist or dry isentropic surfaces are relevant. The idealized GCM simulations discussed in section 7 suggest that humidity anomalies propagate poleward and upward along mean moist rather than dry isentropic surfaces. On the other hand, the distributions of probability of last-saturation location calculated by Galewsky et al. (2005) from reanalysis data suggest that dry isentropic surfaces are relevant for unsaturated motions. The generation of subsaturated air by eddy motions involves unsaturated motions downward and equatorward, which could plausibly occur along dry isentropic surfaces. The inflection points of saturation specific humidity on dry isentropic surfaces would then be convenient markers of the regions in which eddy downward motions are efficient in generating subsaturated air. Further work is needed to determine which dry or moist isentropic surfaces are most appropriate for advection–condensation modeling.

6. Value of the relative humidity minimum

We now consider the effect of other changes in the profile of saturation specific humidity on the degree of

---

[2] On some dry isentropes (particularly in the Northern Hemisphere in summer), there is more than one inflection point in a given hemisphere. We resolve the ambiguity by showing the inflection point corresponding to the maximum rate of poleward decrease in saturation specific humidity. We focus on the DJF season in which identification of the appropriate inflection point in the NH is relatively straightforward. It has previously been noted that the relative humidity minima in Earth's atmosphere are close to the positions of maximum curvature of the zonal-mean dry isentropes (Sherwood et al. 2010b). These positions are not sufficiently different in Earth's atmosphere from the positions given by our inflection point criterion to allow for a strong argument that either criterion is more accurate.

subsaturation in the mean. First, consider the transformations of q_s under which the relative humidity or distance to saturation remain invariant. With the exception of the condensation term, the equation governing the specific humidity [(5)] is linear in specific humidity and depends on derivatives of specific humidity rather than the specific humidity itself. The condensation term may be viewed as the negative of the sum of all other tendency terms conditioned on $q = q_s$ and the sum being positive (cf. O'Gorman and Schneider 2006). Therefore, for a given solution $q(y, t)$ corresponding to a saturation specific humidity profile $q_s(y)$, we can generate a new solution $aq(y, t) + b$ for a saturation specific humidity profile $aq_s(y) + b$, where a and b are constants. The new solution will be a valid solution if the boundary conditions of the problem are compatible and evaporation sources are also rescaled appropriately. The new solution will have the same distance to saturation, but the relative humidity $r = q/q_s$ will be different unless $b = 0$. Neither the relative humidity nor the distance to saturation remains invariant if the boundary conditions or evaporative sources do not change consistently with the linear transformation of q_s.

Consider now the particular case of changes in the meridional gradient of saturation specific humidity, specified through changes in the value of q_s^p (Fig. 8a). Increasing q_s^p leads to a decrease in the meridional gradient of saturation specific humidity, which results in an increase in the relative humidity (Fig. 8b), a decrease in the meridional moisture flux (Fig. 8c), and a decrease in the extratropical condensation rate (Fig. 8d). The decreases in moisture flux and condensation rate might be expected given their direct dependence on meridional moisture gradients according to (A1) and (A2).

It is obvious that increasing q_s^p while holding the equatorial saturation specific humidity fixed must increase the relative humidity, since $q_s^p > 0$ provides the lower bound on the specific humidity q in the model and $r = q/q_s$. This line of reasoning only partly explains the increases in relative humidity; even if q_s^p is held fixed and the equatorial saturation specific humidity q_s^e is instead decreased, the relative humidity still shows an increasing trend. The arguments above regarding linear transformations of q and q_s under which relative humidity is invariant cannot be applied here because the evaporation source is held fixed as q_s is changed.

In summary, the relative humidity distribution remains invariant in our model if the saturation specific humidity distribution and evaporation source are simply rescaled by a constant, but our discussion makes clear that other changes to the saturation specific humidity distribution and evaporation source may affect the relative humidity.
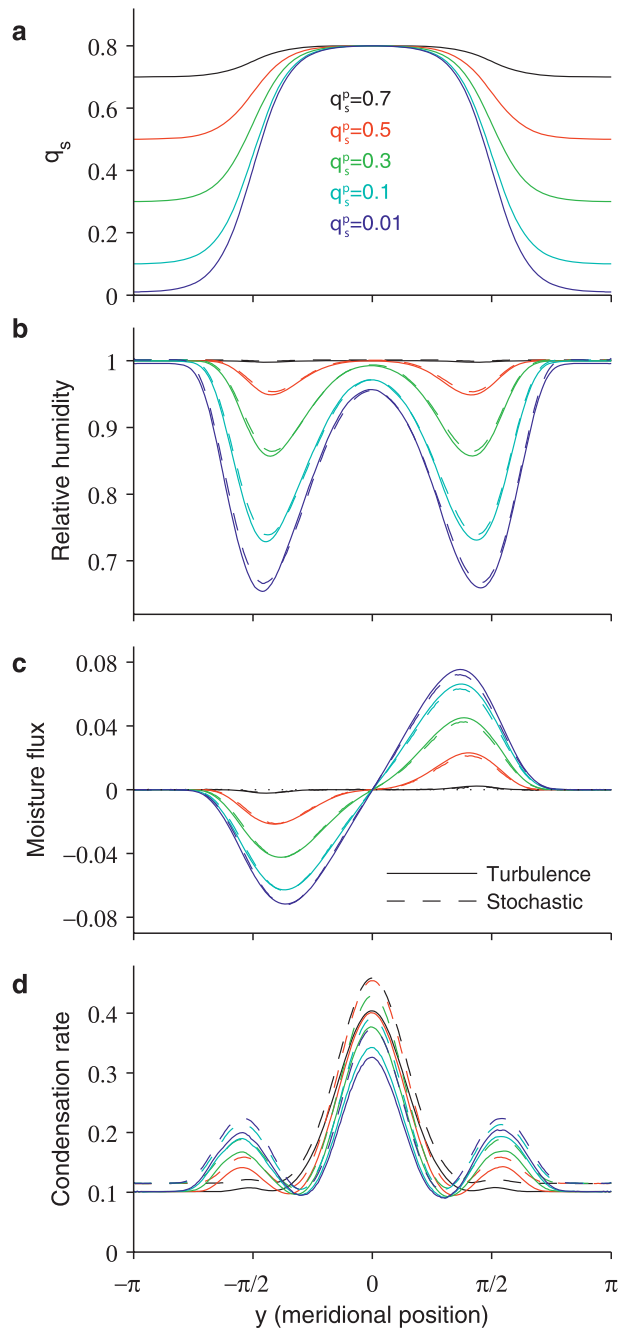

FIG. 8. (a) Variations in the saturation specific humidity profile resulting from changes in the polar saturation specific humidity parameter q_s^p and the resulting mean fields in the turbulence model (solid lines) and stochastic model (dashed lines): (b) RH, (c) meridional specific humidity flux, and (d) condensation rate.

7. Poleward influence of relative humidity in an idealized GCM

It is reasonable to ask whether the limited poleward influence of relative humidity found in simulations with the advection–condensation models would also occur in

an atmosphere that includes latent heat release and temporal variations in saturation specific humidity. Here, we perform a test of the poleward influence of relative humidity in an idealized GCM in which there is an active hydrological cycle but no water vapor radiative feedbacks (O'Gorman and Schneider 2008). The idealized GCM employs a large-scale condensation scheme and a version of the moist convection scheme described in Frierson (2007) and is similar to the GCM introduced by Frierson et al. (2006). The mean thermal structure of the control simulation [corresponding to the reference simulation in O'Gorman and Schneider (2008)] differs from that of Earth's atmosphere primarily because of a lack of ocean heat transports and because of the idealized radiative heating (Fig. 9a). The relative humidity distribution is also different from that of Earth's atmosphere, although there are still pronounced subtropical minima that lie close to the inflection points of saturation specific humidity on dry isentropes. (There are no such inflection points on moist isentropes in much of the troposphere).

We introduce a mean humidity perturbation by changing a parameter in the moist convection scheme in a latitude band around the equator. The parameter specifies the value of the atmospheric relative humidity to which the moist convection scheme relaxes when it is active; it has a default value of 0.7. In the perturbation simulation it is changed to a higher value of 0.8 for grid points within 20° of latitude of the equator. This approach has the advantage that it does not affect energy conservation or the moist adiabatic lapse rate and so will not directly affect the mean thermal structure. Both the control and perturbation simulations are run to statistical equilibrium, and mean fields are then averaged over 1500 days.

Defining anomalies as the difference between the control and perturbation simulations, we see that the anomalies in the relative humidity field are mostly confined to the latitude band in which they are directly forced (indicated by the vertical lines in Figs. 9b,c). The anomalies that do propagate outside this region seem to do so along moist rather than dry isentropes (surfaces of constant equivalent potential temperature are shown; these are shallower than surfaces of constant saturation equivalent potential temperature). There is a notable lack of propagation along dry isentropes in the lower troposphere (Fig. 9b), while the largest increases in relative humidity are confined by the moist isentropes that just intersect the forced region (the green contours in Fig. 9c). We estimate a limit on poleward influence by finding the latitude on each mean isentrope at which the mean saturation specific humidity is equal to the mean specific humidity on the same isentrope at the edge of the forced region (the edge of the forced region is at roughly 20° latitude in each hemisphere; the limit is shown by thick
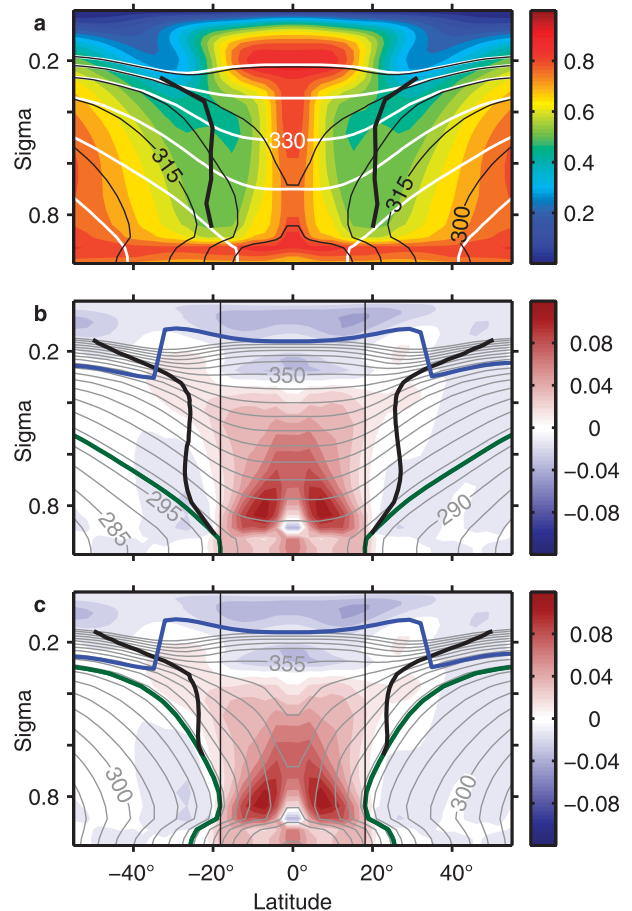

FIG. 9. (a) Zonal- and temporal-mean RH (color shading), dry potential temperature (white contours with interval = 15 K), and equivalent potential temperature (black contours with interval = 15 K) for the control simulation with the idealized GCM. Thick black lines show the inflection points of saturation specific humidity along dry isentropes, calculated as in Fig. 1. (b) Difference in zonal- and temporal-mean RH between the control and perturbation simulations (color shading), and dry potential temperature in the control simulation (gray contours with interval = 5 K). Vertical black lines indicate the extent of the latitude band in which the convection scheme parameter was altered. Thick green lines highlight the mean isentrope that just intersects this latitude band. Thick black lines give an estimate of the poleward extent of influence of RH from the vertical black lines (see text). The thick blue line is the tropopause based on a lapse-rate criterion of 2 K km^{-1}. (c) As in (b), but with equivalent potential temperature contours and with the estimate of poleward influence based on moist isentropic surfaces. Interhemispheric asymmetry in all fields is due to sampling error.

black lines in Figs. 9b,c. Although weak anomalies extend beyond this limit, it provides a reasonable rough estimate of the extent of poleward influence.

Anomalies are also induced in the temperature field, but these are relatively small. Similar results are obtained if we instead plot the change in mean specific humidity normalized by the mean saturation specific humidity in

the control simulation, although with a slightly greater degree of poleward propagation. We also investigated the effects of changing the convection scheme parameter in wider or narrower latitude bands about the equator. In all cases, the anomalies seem to propagate along moist isentropic surfaces. With regard to poleward influence of relative humidity, it is difficult to definitively interpret the results and compare between simulations because of the substantial spatial variations in the activity of parameterized convection, spatial variations in meridional eddy velocity variance, and induced changes in mean vertical velocity in the case of narrow perturbed latitude bands.

8. Conclusions

We have analyzed the behavior of the mean relative humidity distribution along an isentropic surface in an idealized model with a primarily tropical evaporation source. By varying the tropical source amplitude and the profile of saturation specific humidity, we have gained insight into controls on the relative humidity minima and the extent to which humidity at low latitudes affects humidity at higher latitudes.

The first principal result of our study is that condensation introduces a constraint on the poleward influence of the relative humidity field. The distance to saturation at a given location gives the equatorward extent of the domain of dependence of relative humidity at that location; there is little poleward influence of the relative humidity field when the distance to saturation is small. A lack of poleward influence of relative humidity in more realistic atmospheres would have important implications. For example, if the relative humidity is incorrect in a climate model simulation in the deep tropics (possibly because of difficulties parameterizing deep convection), a lack of poleward influence suggests that this error would not directly propagate very far poleward. Equatorward influence may also be small in practice because of low concentrations of water vapor farther poleward. Our advection–condensation model simulations also suggest that the poleward moisture flux is not greatly affected by changes in the tropical evaporation source—a direct consequence of the mean moisture gradient not changing substantially in midlatitudes in response to tropical evaporation changes. In energetic terms, the poleward latent energy flux would not be directly affected by increases in evaporation that are limited to the deep tropics.

The applicability of the lack of poleward influence of relative humidity to the atmosphere is potentially limited by two factors. First, the mean humidity field in the advection–condensation model approaches saturation at the poles, which automatically implies a small distance to saturation even when the gradient of specific humidity

along an isentrope is not large. By contrast, the troposphere at high latitudes has both mean subsaturation and relatively shallow isentropic slopes (Fig. 1). Therefore, the lack of poleward influence may be artificially strong in our model at high latitudes. Second, in more realistic atmospheres the pressure field on isentropic surfaces varies so that the saturation specific humidity is not fixed in time. Our results should still be applicable to the extent that poleward-moving air also cools adiabatically, but again the idealized nature of the model may lead to an exaggeration of the lack of poleward influence of relative humidity.

We have conducted simulations with an idealized GCM to test the extent of poleward influence of relative humidity. The results suggest that anomalies in mean relative humidity in the tropics do not directly lead to strong anomalies in relative humidity in the extratropics. The propagation that does occur seems to occur along moist isentropic surfaces; the steepness of these isentropic surfaces in the tropics is part of the reason for the lack of poleward influence in the simulations, since the moist isentropes approach the tropopause before extending very far poleward. The results of the idealized GCM simulations are not conclusive regarding the role of condensation in limiting poleward influence. Further work might involve devising a different means of inducing relative humidity changes in the GCM (not involving the convection scheme) so that the extent of poleward influence at a range of different levels and latitudes can be examined.

We have also discussed how the relative humidity minima are located near the inflection points of saturation specific humidity in the advection–condensation model, even as the positions of the inflection points are varied. Consistently, the positions of the relative humidity minima did not change in the other sets of experiments in which the tropical evaporation source and meridional saturation humidity gradients changed but the inflection points of the saturation specific humidity profile remained fixed. The subtropical relative humidity minima were also shown to lie close to the inflection points of saturation specific humidity on dry isentropes in the ERA-40 and in a simulation with an idealized GCM. An implication of this result is that even disregarding the (important) effects of mean meridional circulations and cross-isentropic vertical advection, the subtropical relative humidity minima are expected to move poleward as the Hadley circulation widens: increases in the width of the Hadley circulation can be expected to lead to concomitant changes in the low-latitude thermal structure (the tropical region of weak temperature gradients expands) and hence lead to a poleward movement of the positions of the saturation specific humidity inflection points (e.g., Held and Hou 1980; Schneider 2006; Seidel et al. 2008; Schneider et al. 2010). But inflection points of

saturation specific humidity do not generally occur along moist isentropic surfaces in the free troposphere, which means that the relevance of the result is dependent on the isentropic surface that should be used. To the extent that the inflection points mark the positions of efficient generation of subsaturated air by eddy equatorward and downward motions, it may be reasonable to calculate the inflection points on dry isentropic surfaces.

Finally, we have discussed how the mean relative humidity remains invariant if the saturation specific humidity is rescaled by a constant and if the boundary conditions and evaporative sources change consistently. This may be seen as the basic reason that relative humidity does not change greatly in response to global warming, to the extent that the warming is uniform and results in a rescaling of the saturation specific humidity field at a roughly constant fractional rate (cf. Held and Soden 2000). Other types of changes to the saturation specific humidity distribution and evaporation source, however, will change the relative humidity. In particular, we showed how a decrease in the saturation specific humidity gradient on isentropes leads to an increase in relative humidity. Changes in the meridional gradient of saturation specific humidity could result from changes in the slope of the relevant isentropic surfaces.

Further tests of the applicability of our results to more realistic atmospheres are desirable. A key open question is whether there exists an isentropic surface (dry or moist) on which advection–condensation modeling may be consistently applied in the presence of latent heating.

APPENDIX A

Expressions for the Mean Moisture Flux and Condensation Rate

O'Gorman and Schneider (2006) derived analytical expressions for the mean meridional moisture flux and mean condensation rate in a model in which the saturation specific humidity is monotonically decreasing in y and extends over an infinite domain. We refer to these expressions throughout the paper and so we briefly describe them here. The expressions were derived for an initial value problem, but the results of O'Gorman and Schneider (2006) suggest that they could be applied to a statistical steady-state moisture distribution by setting

the initial specific humidity equal to the mean specific humidity and by evaluating them after a time τ_i equal to the time scale characteristic of the irreversible mixing of tracers. The Lagrangian advecting velocity was taken to have an autocorrelation time scale that was zero (the Brownian limit) or infinite (the ballistic limit). Evaporation was not taken into account in the derivation. In the ballistic limit, the mean meridional flux of specific humidity is given by

$$\overline{vq} = -\tau_i \overline{v^2} \left[\frac{\partial \overline{q}}{\partial y} - \frac{dq_s}{dy} P(d, t) \right], \qquad (A1)$$

and the mean condensation rate is given by

$$\overline{c} = \tau_i \overline{v^2} \left| \frac{dq_s}{dy} \right| p(d, \tau_i), \qquad (A2)$$

where $d(y)$ is the distance to saturation defined by (10). The probability density function associated with a meridional displacement δy over a time τ_i is denoted $p(\delta y, \tau_i)$ and is assumed to take the Gaussian form

$$p(\delta y, \tau_i) = \frac{1}{(2\pi \overline{v^2} \tau_i^2)^{1/2}} \exp\left[-\frac{(\delta y)^2}{2\overline{v^2} \tau_i^2} \right]. \qquad (A3)$$

The expression for the flux involves the complementary cumulative distribution function of parcel displacements defined by $P(\delta y, \tau_i) = \int_{\delta y}^{\infty} d\xi\, p(\xi, \tau_i)$.

For large distance to saturation d, the moisture flux [(A1)] becomes proportional to the negative of the mean moisture gradient, and the condensation rate given by (A2) is small. Condensation tends to reduce the meridional moisture flux: in the limit of zero distance to saturation, $P(0, \tau_i) = \frac{1}{2}$ and the moisture flux is half what it would be for a noncondensing tracer with the same meridional gradient. The Brownian limit yields expressions with a similar form, but with the notable exception that the meridional moisture flux is diffusive and does not depend on the distance to saturation.

APPENDIX B

Exact Solution for Restoring Boundary Condition

Sukhatme and Young (2011) derived an exact solution to the spatially inhomogeneous advection–condensation problem with Brownian air parcels and no evaporation sources in the interior of the domain. The solution assumes a monotonically decreasing profile of saturation specific humidity $q_s(y)$ with a well-defined inverse $y_s(q)$. Specializing their solution to the case of a deterministic
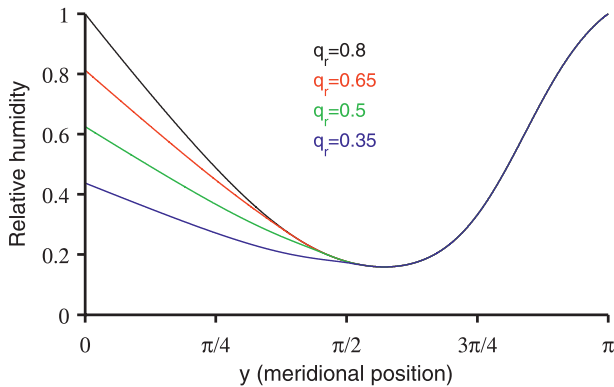
FIG. B1. RH calculated from the exact solution [(B1)] for a range of values of the restoring boundary condition q_r at the equator ($y = 0$). The default saturation specific humidity profile is used (note $q_s = 0.8$ at the equator) but there is no evaporation source in the interior of the domain. All of the solutions are exactly the same sufficiently far poleward.

restoring boundary condition $q = q_r$ at $y = 0$, we find that

$$\bar{r}(y) = \frac{q_m(y)}{q_s(y)} - \frac{y}{q_s(y)} \int_{q_s^p}^{q_m(y)} \frac{1}{y_s(q)} \, dq, \qquad (B1)$$

where $q_m(y) = \min[q_r, q_s(y)]$ and q_s^p is the polar saturation specific humidity value as before. The limited poleward influence of the equatorial boundary condition follows immediately, since for locations sufficiently far poleward that $q_s(y) < q_r$, we have that $q_m(y) = q_s(y)$, and the solution $\bar{r}(y)$ is independent of the boundary value q_r. The poleward influence of the boundary condition is cut off completely at the point at which $q_s(y) = q_r$ [the point at which the distance to saturation defined by (10) becomes infinite].

Evaluating the exact solution [(B1)] for our saturation specific humidity profile [(2)] with default parameters yields the solutions shown in Fig. B1 for a range of values of q_r. The relative humidity minimum occurs close to the inflection point of saturation specific humidity ($y_0 = \pi/2$), but unlike in our simulations it is on the poleward side of the inflection point. The limited poleward influence of the equatorial boundary condition is clearly evident since all the solutions are exactly the same sufficiently far poleward.

REFERENCES

Boer, G. J., and T. G. Shepherd, 1983: Large-scale two-dimensional turbulence in the atmosphere. *J. Atmos. Sci.,* **40,** 164–184.

Bolton, D., 1980: The computation of equivalent potential temperature. *Mon. Wea. Rev.,* **108,** 1046–1053.

Couhert, A., T. Schneider, J. Li, D. E. Waliser, and A. M. Tompkins, 2010: The maintenance of the relative humidity of the subtropical free troposphere. *J. Climate,* **23,** 390–403.

Derbyshire, S. H., I. Beau, P. Bechtold, J. Y. Grandpeix, J. M. Piriou, J. L. Redelsperger, and P. M. M. Soares, 2004: Sensitivity of moist convection to environmental humidity. *Quart. J. Roy. Meteor. Soc.,* **130,** 3055–3079.

Dessler, A. E., and S. C. Sherwood, 2000: Simulations of tropical upper tropospheric humidity. *J. Geophys. Res.,* **105,** 20 155–20 163.

Frierson, D. M. W., 2007: The dynamics of idealized convection schemes and their effect on the zonally averaged tropical circulation. *J. Atmos. Sci.,* **64,** 1959–1976.

——, I. M. Held, and P. Zurita-Gotor, 2006: A gray-radiation aquaplanet moist GCM. Part I: Static stability and eddy scale. *J. Atmos. Sci.,* **63,** 2548–2566.

Galewsky, J., A. Sobel, and I. Held, 2005: Diagnosis of subtropical humidity dynamics using tracers of last saturation. *J. Atmos. Sci.,* **62,** 3353–3367.

Held, I. M., and A. Y. Hou, 1980: Nonlinear axially symmetric circulations in a nearly inviscid atmosphere. *J. Atmos. Sci.,* **37,** 515–533.

——, and B. J. Soden, 2000: Water vapor feedback and global warming. *Annu. Rev. Energy Environ.,* **25,** 441–475.

Hurley, J. V., and J. Galewsky, 2010a: A last saturation analysis of ENSO humidity variability in the subtropical Pacific. *J. Climate,* **23,** 918–931.

——, and ——, 2010b: A last-saturation diagnosis of subtropical water vapor response to global warming. *Geophys. Res. Lett.,* **37,** L06702, doi:10.1029/2009GL042316.

Mitchell, J. F. B., and W. J. Ingram, 1992: Carbon dioxide and climate: Mechanisms of changes in cloud. *J. Climate,* **5,** 5–21.

O'Gorman, P. A., and T. Schneider, 2006: Stochastic models for the kinematics of moisture transport and condensation in homogeneous turbulent flows. *J. Atmos. Sci.,* **63,** 2992–3005.

——, and ——, 2007: Recovery of atmospheric flow statistics in a general circulation model without nonlinear eddy–eddy interactions. *Geophys. Res. Lett.,* **34,** L22801, doi:10.1029/2007GL031779.

——, and ——, 2008: The hydrological cycle over a wide range of climates simulated with an idealized GCM. *J. Climate,* **21,** 3815–3832.

Pierrehumbert, R. T., 1995: Thermostats, radiator fins, and the local runaway greenhouse. *J. Atmos. Sci.,* **52,** 1784–1806.

——, and R. Roca, 1998: Evidence for control of Atlantic subtropical humidity by large scale advection. *Geophys. Res. Lett.,* **25,** 4537–4540.

——, H. Brogniez, and R. Roca, 2007: On the relative humidity of the atmosphere. *The Global Circulation of the Atmosphere,* T. Schneider and A. H. Sobel, Eds., Princeton University Press, 143–185.

Salathé E. P., Jr., and D. L. Hartmann, 1997: A trajectory analysis of tropical upper-tropospheric moisture and convection. *J. Climate,* **10,** 2533–2547.

Schneider, T., 2006: The general circulation of the atmosphere. *Annu. Rev. Earth Planet. Sci.,* **34,** 655–688.

——, and C. C. Walker, 2006: Self-organization of atmospheric macroturbulence into critical states of weak nonlinear eddy–eddy interactions. *J. Atmos. Sci.,* **63,** 1569–1586.

——, K. L. Smith, P. A. O'Gorman, and C. C. Walker, 2006: A climatology of tropospheric zonal-mean water vapor fields and fluxes in isentropic coordinates. *J. Climate,* **19,** 5918–5933.

——, P. A. O'Gorman, and X. Levine, 2010: Water vapor and the dynamics of climate changes. *Rev. Geophys.,* **48,** RG3001, doi:10.1029/2009RG000302.

Seidel, D. J., Q. Fu, W. J. Randel, and T. J. Reichler, 2008: Widening of the tropical belt in a changing climate. *Nat. Geosci.,* **1,** 21–24.

Sherwood, S. C., 1996: Maintenance of the free-tropospheric tropical water vapor distribution. Part II: Simulation by large-scale advection. *J. Climate,* **9,** 2919–2934.

——, W. Ingram, Y. Tsushima, M. Satoh, M. Roberts, P. L. Vidale, and P. A. O'Gorman, 2010a: Relative humidity changes in a warmer climate. *J. Geophys. Res.,* **115,** D09104, doi:10.1029/2009JD012585.

——, R. Roca, T. M. Weckwerth, and N. G. Andronova, 2010b: Tropospheric water vapor, convection, and climate. *Rev. Geophys.,* **48,** RG2001, doi:10.1029/2009RG000301.

Smith, K. S., G. Boccaletti, C. C. Henning, I. Marinov, C. Y. Tam, I. M. Held, and G. K. Vallis, 2002: Turbulent diffusion in the geostrophic inverse cascade. *J. Fluid Mech.,* **469,** 13–48.

Sukhatme, J., and W. R. Young, 2011: The advection-condensation model and water vapour PDFs. *Quart. J. Roy. Meteor. Soc.,* **137,** 1561–1572.

Thomson, D. J., 1987: Criteria for the selection of stochastic models of particle trajectories in turbulent flows. *J. Fluid Mech.,* **180,** 529–556.

Uppala, S. M., and Coauthors, 2005: The ERA-40 Re-Analysis. *Quart. J. Roy. Meteor. Soc.,* **131,** 2961–3012.

Wright, J. S., A. Sobel, and J. Galewsky, 2010: Diagnosis of zonal mean relative humidity changes in a warmer climate. *J. Climate,* **23,** 4556–4569.

Yang, H., and R. T. Pierrehumbert, 1994: Production of dry air by isentropic mixing. *J. Atmos. Sci.,* **51,** 3437–3454.